Digital Signal Processing 34 (2014) 56–66

Contents lists available at ScienceDirect

Digital Signal Processing

www.elsevier.com/locate/dsp

Analysis of local time-frequency entropy features for nonstationary signal components time supports detection

Victor Sucic [a], Nicoletta Saulig [a,*], Boualem Boashash [b,c]

[a] Faculty of Engineering, University of Rijeka, Croatia
[b] College of Engineering, Qatar University, Doha, Qatar
[c] Centre for Clinical Research, University of Queensland, Brisbane, Australia

ARTICLE INFO

Article history:
Available online 24 July 2014

Keywords:
Time-frequency
Rényi entropy
Spectrogram
Component number

ABSTRACT

Identification of different specific signal components, produced by one or more sources, is a problem encountered in many signal processing applications. This can be done by applying the local time-frequency-based Rényi entropy for estimation of the instantaneous number of components in a signal. Using the spectrogram, one of the most simple quadratic time-frequency distributions, the paper proves the local applicability of the counting property of the Rényi entropy. The paper also studies the influence of the entropy order and spectrogram parameters on the estimation results. Numerical simulations are provided to quantify the observed behavior of the local entropy in the case of intersecting components. The causes of decrements in the local number of time supports in the time-frequency plane are also studied. Finally, results are provided to illustrate the findings of the study and its potential use as a key step in multicomponent instantaneous frequency estimation.

1. Introduction

Nonstationary signals encountered in engineering applications (civil, military, biomedical) are often characterized by multiple components with varying spectral contents. Different signal components may have overlapping time supports, making the classical time representation inadequate to correctly identify the energy contribution of each component. Similarly, the frequency representation fails to correctly map the spectral energy of different components if they share frequency content. Joint time and frequency representations, being energy distributions showing the signal local frequency content, overcome such limitations of the classical signal representations [1]. These time-frequency distributions allow the isolation of different spectral components that are present in a signal, as well as their respective instantaneous frequencies [2]. The number of components that are present in a signal can thus be visually identified. However, for applications requiring the automated assessment of the number of components, objective criteria are needed.

Applications such as classification, require time-frequency features that can be used for pattern recognition as an aid to identification and detection. A simple but efficient feature is the measure of complexity, which is extensively reviewed in this paper and applied to the estimation of the number of components in a signal.

For blind source separation algorithms, based on peaks extraction and tracking from TFDs, the key information is the local number of components, i.e. the instantaneous number of components supported in time. The recently introduced Short-term Rényi entropy [3] provides reliable information about the time support of different components, and thus can be used as the input information to peak detection and extraction techniques [1,4]. The Short-term Rényi entropy, as an indicator of the local number of time supported components, is discussed in Section 2. The simplified model presented in [3] doesn't clarify the role of the entropy order α and TFD features (local time and frequency supports) in the estimation. The Short-term Rényi entropy when applied to the spectrogram, being a widely used TFD, is therefore studied in Section 2. The analysis of particular situations occurring in nonstationary signals (ending/starting component, overlapping or intersecting components) is essential for correctly interpreting the information provided by the Short-term Rényi entropy, as explained in Section 3. Experimental results are provided in Section 4. In Section 5, the obtained results are discussed, and possible prospectives are considered.

* Corresponding author at: Faculty of Engineering, University of Rijeka, Vukovarska 58, 51000, Rijeka, Croatia.
E-mail addresses: vsucic@riteh.hr (V. Sucic), nsaulig@riteh.hr (N. Saulig), boualem@qu.edu.qa (B. Boashash).

http://dx.doi.org/10.1016/j.dsp.2014.07.013
1051-2004/

2. The Short-term Rényi entropy and the local component number estimation

2.1. The Rényi entropy of time-frequency distributions

Let's consider a multicomponent analytic signal with M components defined as

$$x(t) = \sum_{k=1}^{M} x_k(t), \tag{1}$$

with each of its component having the form

$$x_k(t) = a_k(t) e^{j\phi_k(t)}, \tag{2}$$

where $a_k(t)$ is the signal instantaneous amplitude, while the signal instantaneous frequency (IF) is defined as the time derivative of its instantaneous phase $\phi_k(t)$ [2]

$$f_k(t) = \frac{1}{2\pi}\frac{d\phi_k(t)}{dt}. \tag{3}$$

TFDs are expected to have highly resolved spectral components, while minimizing interferences. Maintaining highly concentrated components, while suppressing interferences [5] is a demanding task in the design of TFDs [6–10]. TFDs belonging to the Quadratic class are defined as [1,11]:

$$\rho_x(t,f) = \int_{-\infty}^{\infty}\int_{-\infty}^{\infty}\int_{-\infty}^{\infty} g(\nu,\tau) x\left(t+\frac{\tau}{2}\right) x^*\left(t-\frac{\tau}{2}\right) \times e^{j2\pi(\nu t - \nu u - f\tau)}\, du\, d\nu\, d\tau, \tag{4}$$

where $g(\nu,\tau)$ is the TFD kernel filter that defines the TFD and its properties. Some of the properties satisfied by the Quadratic TFDs, i.e. the preservation of the global signal energy in the (t,f) plane [1]

$$\int_{-\infty}^{\infty}\int_{-\infty}^{\infty} \rho_x(t,f)\, dt df = E_x, \tag{5}$$

and the time and frequency marginal conditions

$$\int_{-\infty}^{\infty} \rho_x(t,f)\, df = \left|x(t)\right|^2, \tag{6}$$

$$\int_{-\infty}^{\infty} \rho_x(t,f)\, dt = \left|X(f)\right|^2, \tag{7}$$

allow for a possible interpretation of a TFD as a pseudo-probability density function.

These assumptions allow the application of complexity measures from information theory to TFDs, such as the generalized entropy of Rényi [12]:

$$H_{\alpha,x} := \frac{1}{1-\alpha}\log_2 \int_{-\infty}^{\infty}\int_{-\infty}^{\infty} \left(\frac{\rho_x(t,f)}{\int_{-\infty}^{\infty}\int_{-\infty}^{\infty}\rho_x(t,f) df dt}\right)^{\alpha} dt\, df, \tag{8}$$

where the parameter α is the order of the Rényi entropy.

A useful property of the Rényi entropy is its counting property. If an ideal TFD, $I_x(t,f)$, of a two-component signal, $x(t) = x_1(t) + x_2(t)$ (where $x_2(t)$ is the time and/or frequency shifted copy of $x_1(t)$, and their respective TFDs are defined as $I_{x_1}(t,f)$, and $I_{x_2}(t,f)$) is

$$I_x(t,f) = I_{x_1}(t,f) + I_{x_2}(t,f) = I_{x_1}(t,f) + I_{x_1}(t-t_0, f-f_0), \tag{9}$$

then, the Rényi entropy of such TFD will result into

$$H_{\alpha,x_1+x_2} = \frac{1}{1-\alpha} \times \log_2 \int_{-\infty}^{\infty}\int_{-\infty}^{\infty} \left(\frac{I_{x_1}(t,f) + I_{x_1}(t-t_0,f-f_0)}{\int_{-\infty}^{\infty}\int_{-\infty}^{\infty} I_{x_1}(t,f) + I_{x_1}(t-t_0,f-f_0) df\, dt}\right)^{\alpha} dt\, df. \tag{10}$$

Under the assumption that $I_{x_1}(t,f)$ and $I_{x_1}(t-t_0, f-f_0)$ are compactly supported non-overlapping components in the (t,f) plane, the Rényi entropy will carry exactly one more bit of information when compared to the Rényi entropy of the TFD of one of the components [13], i.e.

$$H_{\alpha,x_1+x_2} = H_{\alpha,x_1} + 1 = H_{\alpha,x_2} + 1, \tag{11}$$

so that the number of components $M = 2$ can be estimated as

$$N = 2^{H_{\alpha,x_1+x_2} - H_{\alpha,x_1}} = 2^{H_{\alpha,x_1+x_2} - H_{\alpha,x_2}} = 2. \tag{12}$$

In general, the number of estimated components N, in an M component signal with non-overlapping components, being represented by an ideal TFD, can be determined as

$$N = 2^{H_{\alpha,x_1+x_2+\ldots+x_M} - H_{\alpha,x_m}} = M, \tag{13}$$

where $x_m(t)$ is an arbitrarily chosen component from the mixture. In order for Eq. (13) to hold, all signal components must exhibit the same time and frequency supports, i.e. all components must be replicas of the referent component $x_m(t)$, shifted in time and/or frequency [3,13]. Additionally, the reference components must be known by the signal analyst. These assumptions do not hold in general.

Recently, the Short-term Rényi entropy [3] has been introduced in order to overcome the above limitations of the global Rényi entropy as an estimator of the number of signal components. The Short-term Rényi entropy approach can precisely estimate the number of components that are present in a short time interval of a TFD, even for signals whose components present different time and frequency supports, and without prior knowledge of the signal as shown in [3,14].

Since the effective application of the global Rényi entropy requires signals whose components have equal time and frequency supports, the estimation by the local Rényi entropy exploits the fact that locally, in a short time interval Δt of a TFD, different components have equal frequency supports [3].

2.2. The stationary signal model

One of the most routinely used TFDs is the intuitive spectrogram, obtained as the squared magnitude of the Short-time Fourier transform (STFT). The kernel filter of the spectrogram can be expressed as [1]:

$$g(\nu,\tau) = \mathcal{F}_{t\to\nu}\left\{ w\left(t+\frac{\tau}{2}\right) w\left(t-\frac{\tau}{2}\right)\right\} = A_w(\nu,\tau), \tag{14}$$

where $w(t)$ is the analysis window used in the Short-time Fourier transform.

However, the spectrogram suffers from limited time-frequency resolution, determined by the time and frequency supports of the

window $w(t)$. Despite this disadvantage, its simple definition, strict positivity, realness, and appearance of interferences only in the case of spectral overlapping of different components, make it suitable in some cases for the representation of nonstationary signals, as well as for theoretical analysis, if the analysis window is optimally selected.

2.2.1. Case of a pure tone

In this study, the behavior of the locally applied Rényi entropy is illustrated on the example of a pure tone

$$x(t) = e^{j2\pi f_0 t}. \tag{15}$$

The STFT of this signal, modulated with a Gaussian window $w(t) = (\pi\sigma^2)^{-1/4} e^{-t^2/2\sigma^2}$, is expressed as [15] (see Proof 1 in Appendix A):

$$STFT_x(t, f) = \left(\pi\sigma^2\right)^{-1/4} \sqrt{2\sigma^2\pi}\, e^{-j2\pi(f-f_0)t} e^{\frac{-4\pi^2\sigma^2(f-f_0)^2}{2}}. \tag{16}$$

Hence the signal spectrogram becomes

$$S_x(t, f) = K e^{-4\pi^2\sigma^2(f-f_0)^2}, \tag{17}$$

with $K = 2\sqrt{\pi}\sigma$.

The time slice to be analyzed is obtained by annulling the spectrogram outside a time interval Δt, centered around the instant p, as given by Eq. (18)

$$Sp_x(t, f) = \begin{cases} S_x(t, f), & p - \Delta t/2 < t < p + \Delta t/2 \\ 0, & \text{otherwise.} \end{cases} \tag{18}$$

The Rényi entropy of Eq. (18) is

$$H_{\alpha,x}(p) = \frac{1}{1-\alpha} \times \log_2 \int_{p-\Delta t/2}^{p+\Delta t/2} \int_{-\infty}^{\infty} \left(\frac{K e^{-4\pi^2\sigma^2(f-f_0)^2}}{\int_{p-\Delta t/2}^{p+\Delta t/2} \int_{-\infty}^{\infty} K e^{-4\pi^2\sigma^2(f-f_0)^2}\, dt\, df} \right)^{\alpha} dt\, df, \tag{19}$$

resulting in (see Proof 2 in Appendix A):

$$H_{\alpha,x}(p) = \log_2 \Delta t + \log_2 \frac{1}{2\sqrt{\pi}\sigma} \alpha^{-\frac{1}{2(1-\alpha)}} = \log_2 \Delta t + \log_2 \frac{1}{K} \alpha^{-\frac{1}{2(1-\alpha)}}. \tag{20}$$

Eq. (20) shows that the local entropy of the spectrogram time slice of a pure tone depends on the duration of the interval Δt, the characteristics of the spectrogram window $w(t)$, and the order of the Rényi entropy α. In fact, the value of the first term of Eq. (20) depends on the local time support of the component, which is determined by the choice of the analyzing interval of the local entropy. The second term contains the parameters that control the characteristics of the normalized time slice of the TFD taken to the power α. The concentration of the time slice of the TFD is controlled by the standard deviation σ of the spectrogram window, and is additionally enhanced by taking the slice to the power of α. The second term of Eq. (20) can thus be split into two terms in order to independently analyze the influence of the spectrogram parameter σ and the entropy order α:

$$H_{\alpha,x}(p) = \log_2 \Delta t + \log_2 \frac{1}{K} + \log_2 \alpha^{-\frac{1}{2(1-\alpha)}}. \tag{21}$$

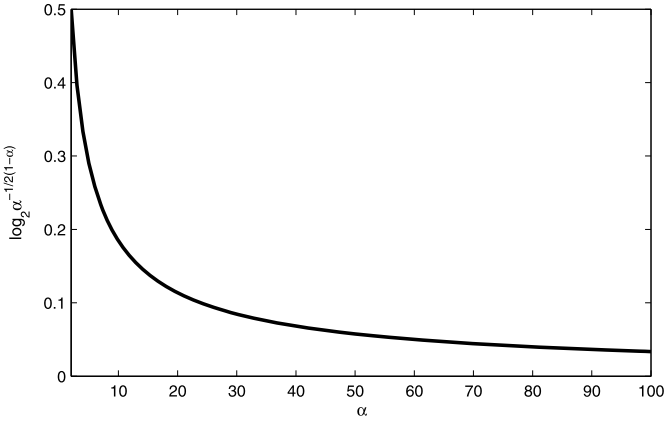

Fig. 1. Dependency of the third term of Eq. (21) on the entropy order α.

Eq. (21) shows that the local Rényi entropy exhibits an unbounded decrease as the parameter σ increases. Higher entropy orders increase the peakedness of the analyzed TFD slice, having the effect of decreasing the total slice entropy. However, the value of the third term of Eq. (21) decreases as the entropy order α increases, as shown in Fig. 1, since for $\lim_{\alpha\to\infty} \alpha^{-\frac{1}{2(1-\alpha)}} = 1$.

As expected, the local entropy is invariant to changes in the signal frequency f_0, and for fixed values of the entropy analyzing window Δt, the entropy order α, and the spectrogram parameter σ, the local entropy is constant for each time instant p.

2.2.2. Case of a two-component signal

In the case of a two component signal, with the components being shifted versions of the reference signal $x(t)$, i.e.

$$x_1(t) = x(t - t_1) e^{j2\pi f_{1'} t} \quad \text{and} \quad x_2(t) = x(t - t_2) e^{j2\pi f_{2'} t}, \tag{22}$$

where $f_0 + f_{1'} = f_1$, and $f_0 + f_{2'} = f_2$, the spectrogram can be expressed as [15]

$$S_{x_1+x_2}(t, f) = K e^{-4\pi^2\sigma^2(f-f_1)^2} + K e^{-4\pi^2\sigma^2(f-f_2)^2} - 2K e^{-2\pi^2\sigma^2[(f-f_1)^2+(f-f_2)^2]} \times \cos\left[2\pi(f_1 - f_2)t + \Phi + \pi\right]. \tag{23}$$

The cosine in the third term of the summation is a scaling factor that represents the overlapping spectral content of the components; its argument is dependent on the spectral distance of the two components and their initial phases.

The model from which the global Rényi entropy counting property has been derived [13] assumes compactly supported components, and a quasi-linear TFD, implying that the components don't share energy content in the (t, f) plane. However, for the theoretic model in Eq. (23), where a Gaussian window has been used for the realization of the spectrogram, the components will not have compact support in frequency. However, by assuming that the frequencies f_1 and f_2 are distant enough so that the spectral characteristics of $w(t)$ do not cause significant component overlapping in the (t, f) plane, the third term of Eq. (23) can be neglected.

By observing a time slice of duration Δt of the spectrogram in Eq. (23), the local entropy in Eq. (8) will result into:

$$H_{\alpha,x_1+x_2}(p) \approx \log_2 \Delta t + \log_2 \frac{1}{K} \alpha^{-\frac{1}{2(1-\alpha)}} + 1. \tag{24}$$

The comparison of Eqs. (21) and (24) indicates that the local Rényi entropy of the two component signal spectrogram carries approximately one more bit of information when compared to the entropy of the time slice of the reference component spectrogram. Hence, the counting property of the Rényi entropy can be applied locally

in order to obtain the instantaneous number of components in a multicomponent signal as:

$$N(p) = 2^{H_{\alpha,x_1+x_2}(p) - H_{\alpha,x}(p)} \approx 2^1, \tag{25}$$

and in general

$$N(p) = 2^{H_{\alpha,x_1+x_2+\ldots+x_M}(p) - H_{\alpha,x}(p)} \approx M(p). \tag{26}$$

By computing N for each time instant p, a continuous function representing the local number of components is then obtained.

Eqs. (21) and (24) imply that Eq. (26) holds only by selecting the same parameters σ and α for the analyzed multicomponent and the reference signal. In other words, the estimated number of components $N(p)$ is then invariant to the spectral characteristics of the analyzed and reference signals. In fact, Eq. (26) holds since the equal parameters used to generate the TFDs of the analyzed and reference signals guarantee same frequency supports. The same entropy order α yields the same shapes of the time slices of the TFDs of the analyzed and reference signals; they are the time slices over which the integrations in Eq. (8) are performed. Under these conditions, the counting property of the Rényi entropy holds locally.

Note that for $\alpha = 1$ the generalized Rényi entropy reduces to Shannon entropy [1]. In this case, from Eqs. (21) and (24) we have

$$\lim_{\alpha\to 1} H_{\alpha,x}(p) = \log_2 \Delta t + \log_2 \frac{1}{K} + \log_2 \sqrt{e}, \tag{27}$$

and

$$\lim_{\alpha\to 1} H_{\alpha,x_1+x_2}(p) \approx \log_2 \Delta t + \log_2 \frac{1}{K} + \log_2 \sqrt{e} + 1. \tag{28}$$

Thus, the local counting property also holds for Shannon entropy.

2.2.3. The case of completely overlapping components in the time-frequency plane

In the previous analysis, the spectrogram model used to analyze the local entropy has been simplified by assuming that the components were enough disclosed in frequency to minimize interferences. On the other hand, when two stationary components, Eq. (22), completely overlap in the (t, f) plane, that is $f_1 = f_2$, the local Rényi entropy takes the form:

$$H_{\alpha,x_1+x_2}(p) = \frac{1}{1-\alpha} \times \log_2 \int_{p-\Delta t/2}^{p+\Delta t/2} \int_{-\infty}^{\infty} \left(\frac{2KK_1 e^{-4\pi^2\sigma^2(f-f_1)^2}}{\int_{p-\Delta t/2}^{p+\Delta t/2} \int_{-\infty}^{\infty} 2KK_1 e^{-4\pi^2\sigma^2(f-f_1)^2}\, dt\, df} \right)^{\alpha} dt df, \tag{29}$$

where $K_1 = 1 - \cos(\Phi + \pi)$.

Eq. (29) indicates that an equivalent situation to the case of a single component (Eq. (19)) is obtained, since the term K_1 is a constant scaling factor. It follows that for two completely overlapped components, even in the case when $\Phi = \pi(2n+1)$, $n \in Z$

$$\lim_{\Phi\to\pi} H_{\alpha,x_1+x_2}(p) = \log_2 \Delta t + \log_2 \frac{1}{K} \alpha^{-\frac{1}{2(1-\alpha)}} = H_{\alpha,x}(p), \tag{30}$$

and

$$N(p) = 2^{H_{\alpha,x}(p) - H_{\alpha,x}(p)} = 2^0 = 1. \tag{31}$$

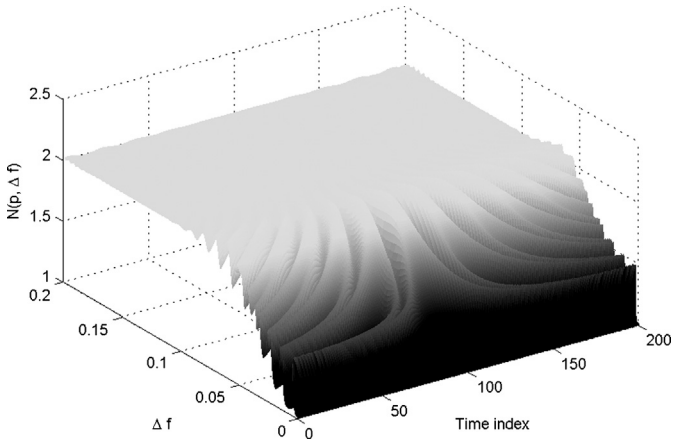

Fig. 2. Number of components $N(p)$ w.r.t. the frequency separation Δf between two stationary components.

2.2.4. The case of partially overlapping components in the time-frequency plane

When the shared spectral content of two components cannot be neglected, meaning that the two components partially overlap, but so that $f_1 - f_2 \neq 0$, based on Eq. (23) the local Rényi entropy, and thus the local number of components, will exhibit a periodic behavior depending on the period of the interference term. From Eq. (23) it can be seen that the estimated number of components $N(p)$ in the case of partially overlapping components will depend on the amount of the shared spectral content (determined by the standard deviation σ of the window $w(t)$, and by $\Delta f = f_1 - f_2$), the time instant t, and the phase difference Φ.

Fig. 2 shows the estimated number of components $N(p)$ in the case of two components with gradually decreased Δf, and $\Phi = 0$. It can be noticed that from an initial constant value $N(p, \Delta f) = 2$ (when Δf is large enough to avoid spectral interferences), the estimated number of components presents an oscillatory transition region bandwidth, whose period is proportional to Δf, until $N(p, \Delta f)$ approaches 1 as $\Delta f \to 0$. Clearly, the transition period can be shorten by increasing the value of σ.

2.3. The nonstationary signal model

2.3.1. The spectrogram model

Eq. (26) has been derived for the model of the spectrogram of stationary signals. However, the local estimation can generally be applied to nonstationary signals. The aim of the entropy estimation is to precisely determine the local number of components, for which a good time resolution is needed. When estimating the local number of components in nonstationary signals, the spectrogram window should be chosen short enough to isolate only the local spectral content of each component. This requirement will be met by a spectrogram with the window $w(t)$ that isolates only a small portion of the analyzed signal, such that the spectral characteristics of the signal are locally stationary. Therefore, the spectrogram of a nonstationary signal can locally be replaced by the stationary model, making Eq. (23) generally applicable to nonstationary signals:

$$S_{x_1+x_2}(t, f) \approx Ke^{-4\pi^2\sigma^2(f-f_1(t))^2} + Ke^{-4\pi^2\sigma^2(f-f_2(t))^2} - 2Ke^{-2\pi^2\sigma^2[(f-f_1(t))^2+(f-f_2(t))^2]} \times \cos\left[2\pi\left(f_1(t) - f_2(t)\right)t + \Phi + \pi\right]. \tag{32}$$

By supposing that the two nonstationary components are disclosed enough to avoid significant interferences, meaning that the third term in Eq. (32) can be neglected, Eq. (24) can be adapted also

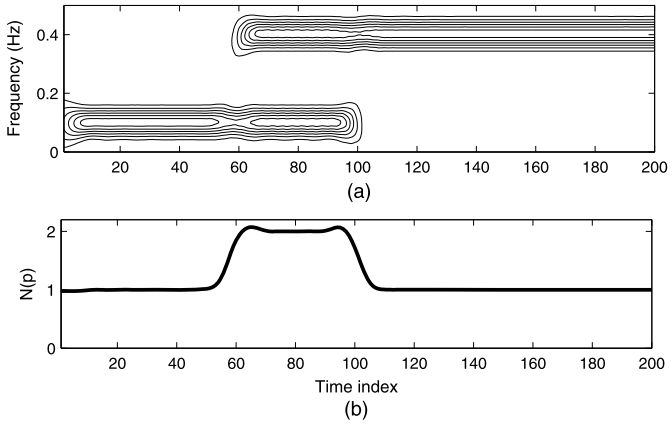

Fig. 3. Spectrogram of a two component signal with stationary components (a), estimated number of components $N(p)$ (b).

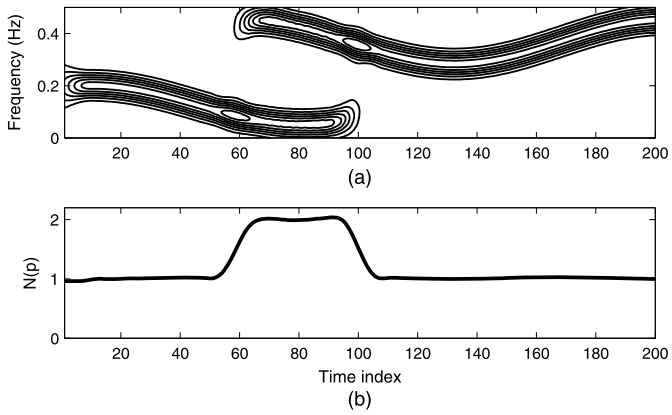

Fig. 4. Spectrogram of a two component signal with nonstationary components (a), estimated number of components $N(p)$ (b).

for nonstationary signals (since the time dependencies of the instantaneous frequencies $f_1(t)$ and $f_2(t)$ disappear under frequency integration, see Proof 2 in Appendix A). This shows that the counting property of the Rényi entropy, Eq. (26), can locally be applied to nonstationary signals. Furthermore, the invariance of the Rényi entropy (under the condition of locally quasi-stationary signals) on the time dependency of the instantaneous frequencies $f_1(t)$ and $f_2(t)$, allows the maintenance of the same reference signal Eq. (15) as in the stationary case. The reference signal can thus be synthetically created as a sinusoid (with arbitrarily chosen amplitude and frequency), to which the Hilbert transform is applied to obtain the form as in Eq. (15).

Figs. 3 and 4 compare the results of the local entropy estimation on the examples of the spectrograms of a pair of two-component signals, with stationary and nonstationary components, respectively. Both the stationary and nonstationary components have same time supports. Similar estimation result have been obtained, confirming that the nonstationarity does not affect the local entropy estimation.

2.3.2. Local overlapping of nonstationary components

When two components are well separated in the (t, f) plane, the third term in Eq. (29) can be omitted, and hence the estimated number of components will be equal to two, independent of $f_1(t)$ and $f_2(t)$.

On the other hand, when an intersection of two nonstationary components occurs at a time instant t_0, $(f_1(t_0) = f_2(t_0))$, if the time interval Δt is short enough that the frequencies $f_1(t)$ and $f_2(t)$ can be considered constant $(f_1(t) \approx f_1$, and $f_2(t) \approx f_2$ inside $\Delta t)$, the obtained function $N(p)$ can ideally be represented by a cross-cut of the plane $N(p, \Delta f)$ (Fig. 2), by the plane $\Delta f(p) = |f_1(p) - f_2(p)|$. However, such representation is a rough approximation, and at the instant of the components intersection t_0 the estimated number of components, centered around the time instant $p = t_0$, is approximately equal to one (since the condition $f_1(t) = f_2(t)$ holds only for the time instant t_0, inside the entropy analyzing interval Δt).

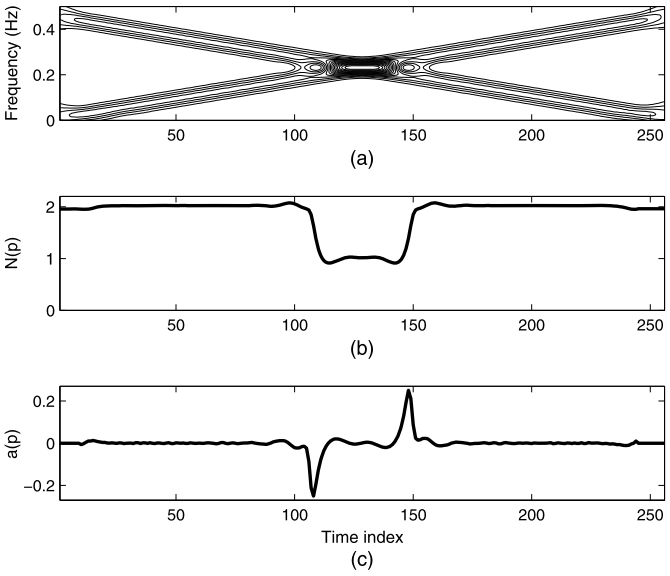

Fig. 5. Spectrogram of a two component signal with crossing components (a), estimated number of components $N(p)$, numerical derivative of $N(p)$ (c).

In general, when an intersection of the components IFs occurs inside the interval Δt, the estimated number of components of a multicomponent signal will be:

$$N(p) \approx M(p) - 1. \tag{33}$$

Thus, even when $M(p)$ components are supported in time and contributing to the local spectrum, the local entropy detects only the number of different regions of the (t, f) plane occupied by the signal. Fig. 5(a) and Fig. 5(b) show the spectrogram of a signal having two crossing components and the corresponding estimated number of components $N(p)$.

3. Some ambiguous situations in the time-frequency plane

3.1. The first derivative of $N(p)$ as a classification feature

Besides the case when two nonstationary components intersect, as in Fig. 5, the local number of components, estimated using the Rényi entropy, also decreases when one of the components stops and another component starts, as shown in Fig. 6. However, these two different situations should be distinguished in order to correctly establish the time supports of all components. Even though the distinction of these two situations may visually appear trivial, computational solutions are not, as they are based on the counting of the local number of peaks, rather than the regions occupied by the signal in the (t, f) plane. In fact, when two components intersect, the local number of peaks decreases, same as in the case when one component stops. So there is no additional information to indicate the local number of components supported in time (which may be interpreted as the number of active signal sources in one time instant). Indeed, this information is essential for a complete extraction of two intersecting components.

Algorithms for components extraction [4,16] rely on the information of the local number of components obtained from the

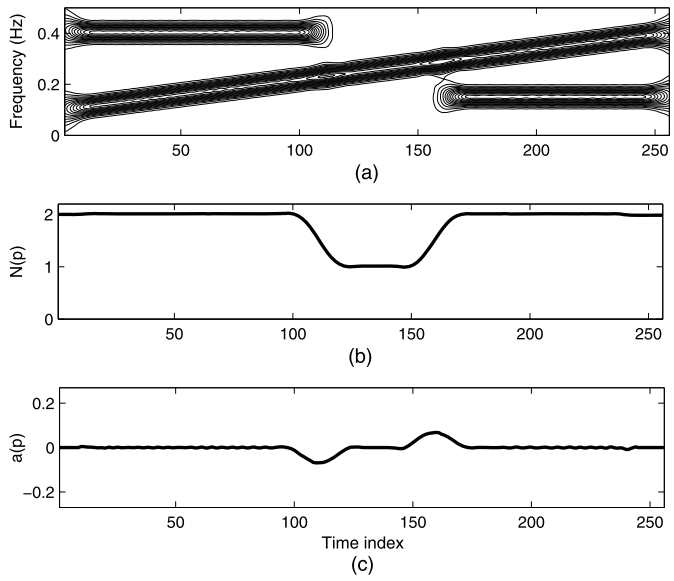

Fig. 6. Spectrogram of a three component signal with truncated components (a), estimated number of components $N(p)$, and numerical derivative of $N(p)$ (c).

counting of the local peaks in a time slice of a TFD, in order to extract sequentially different components from the TFD. Since from the counting of the local peaks in a time slice of a TFD information on the components intersections cannot be provided, the extraction algorithms proposed in [4,1,16] are limited to classes of signals with non-intersecting component, or signals in which all components have same time supports (with an assumption that each decrement in the local number of peaks is a component intersection).

When comparing the estimation results in Figs. 5 and 6, it becomes apparent that the estimated number of components $N(p)$ changes much faster when the components intersect than in the case when one component ends. This claim is validated by the fact that the ending and starting components of the signal in Fig. 6 have been sharply truncated by a rectangular window to simulate the fastest possible change of $N(p)$ inside the entropy analyzing interval Δt. However, due to the non-ideal time localization in practical TFDs, whenever one component ends, its energy spreads over a time interval, even when the component is sharply truncated. This transition period (from the instant when the component starts to fade, until the instant it disappears) causes the gradual decrease of $N(p)$. If we take into consideration the spectrogram of a signal with one of the components sharply truncated in the time instant t_0 inside the entropy analyzing interval Δt, meaning that $M(p+\Delta t/2) = M(p-\Delta t/2)-1$, then the local Rényi entropy can be written as:

$$
\begin{aligned}
&H_\alpha(p) \\
&= \frac{1}{1-\alpha}\log_2\Bigg[\Bigg(\int_{p-\Delta t/2}^{p+\Delta t/2}\int_{-\infty}^{\infty}\Bigg(\sum_{m=1}^{M(p+\Delta t/2)} K e^{-4\pi^2\sigma^2(f-f_m(t))^2} \\
&\quad + 1_{\Delta t'}(t-p)K e^{-4\pi^2\sigma^2(f-f_{M(p-\Delta t/2)}(t))^2}\Bigg)^{\alpha} dt df\Bigg) \\
&\quad \times\Bigg(\Bigg(\int_{p-\Delta t/2}^{p+\Delta t/2}\int_{-\infty}^{\infty}\sum_{m=1}^{M(p+\Delta t/2)} K e^{-4\pi^2\sigma^2(f-f_m(t))^2} \\
&\quad + 1_{\Delta t'}(t-p)K e^{-4\pi^2\sigma^2(f-f_{M(p-\Delta t/2)}(t))^2} dt df\Bigg)^{\alpha}\Bigg)^{-1}\Bigg], \qquad (34)
\end{aligned}
$$

where

$$
1_{\Delta t'}(t-p) = \begin{cases} 1, & \text{for } t \in [p-\Delta t/2, t_0], \\ 0, & \text{otherwise} \end{cases} \qquad (35)
$$

represents the time support of the truncated component.

Hence, the estimated number of components, while the time instant t_0 is included in the analyzing interval Δt, is:

$$
N(p) = \frac{\Delta t(\frac{2M(p+\Delta t/2)+1}{2}) + t_0 - p}{\Delta t} \qquad (36)
$$

and its first derivative is:

$$
N'(p) = -\frac{1}{\Delta t}. \qquad (37)
$$

In analogy, when one component starts inside the interval Δt, the first derivative of $N(p)$ is:

$$
N'(p) = \frac{1}{\Delta t}. \qquad (38)
$$

Thus, in the case of starting/ending components inside the time interval Δt, the absolute derivative of the function $N(p)$ is

$$
\left|N'(p)\right| = \frac{1}{\Delta t}. \qquad (39)
$$

Clearly, Eq. (32) represents a simplified model, since the spectrogram of a signal will never be sharply truncated, but will rather present a graduate fading inside the duration of the time analyzing window $w(t)$. However, by taking into account the quasi-ideal time localization of the components assured by a short analyzing window $w(t)$, the fading of the component inside the interval Δt can be neglected.

More significant changes in $N(p)$ come from decreases in the local bandwidth that occur when two components intersect (since the bandwidths of two components are reduced to a single bandwidth), as shown in Fig. 5(a), (b). This suggests that the features of the function $N(p)$ may reveal the occurrence of a components intersection in the ambiguous situation of the number of components locally decreasing, by computing the function

$$
a(p) = N(p+1) - N(p), \qquad (40)
$$

which corresponds to the numerical first derivative of $N(p)$. In the case of intersecting components, $N(p)$ is characterized by brusque changes, hence yielding larger values of $a(p)$ than in the case of components rising/fading.

3.2. Criteria validation

In order to establish a numerical criterion to distinguish the situations of components crossing and component ending/starting, the extrema of the function $a(p)$ have been calculated for both cases (by taking into consideration numerous different examples of intersections) for noiseless and noisy conditions.

3.2.1. Numerical example on simulated data

The function $a(p)$ has first been calculated for the case of sharply truncated components. The result shown in Fig. 6 is obtained by using the spectrogram and entropy parameters optimized as in [3]: the spectrogram with a *Gaussian* window of duration $D/10$, $\Delta t = D/17$ (where D is the total number of time samples in the signal), and $\alpha = 7$ in order to suppress the influence of moderate noise (especially important for real-life signals). The extreme values of the numerical derivative of $N(p)$ are $min(a(p)) = -0.066$, and $max(a(p)) = 0.0641$, which are very close to the value of Eq. (39) since $\Delta t = 15$. Since the components are sharply truncated, $min(a(p))$ and $max(a(p))$ represent the smallest

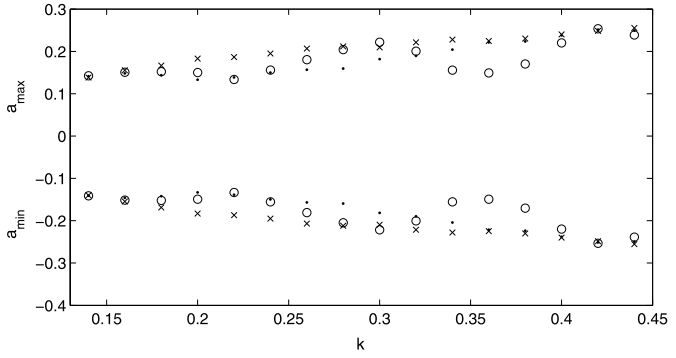

Fig. 7. Extreme values of $a(p)$ w.r.t. the chirp rate k for $t_0 = 0.5$ s ($\cdot$), $t_0 = 0.5781$ s ($\circ$), and $t_0 = 0.5156$ s ($\times$).

and largest possible values of $a(p)$ that can be achieved in the case of ending/starting components for a chosen set of parameters.

To analyze the case of intersecting components, let's consider two LFM components of total duration $T = 1$ s, defined as

$$y_1(t) = e^{j2\pi(\frac{k}{2}t^2+\phi)}$$
$$y_2(t) = e^{j2\pi(kTt-\frac{k}{2}t^2)} \tag{41}$$

In order to simulate a wide range of phase shifts in the intersection time instant for this study, three different simulation sets are selected, such that

$$y_1(t_0) = 1, \quad \text{for } t_0 = 0.5, 0.5156, \text{ and } 0.5781, \tag{42}$$

and $N(p)$ has been calculated by gradually changing the chirp rate k from 0.14 to 0.44, in order to vary the sharp angle defined by the intersecting components from the initial 47.5° to the final 16°, for each of the considered t_0.

The extreme values of $a(p)$ for each simulation are reported in Fig. 7. The numerical results confirm that abrupt changes in the local entropy, and hence in the local number of components $N(p)$, are typical in the case of intersecting components. When components intersections begin/end, considerably larger values of $|a(p)|$ (at least double) can be expected when compared to the case when one of the components ends and another one starts.

Following this criterion, each decrement of $N(p)$ which is preceded and succeeded by values of $|a(p)|$ larger than the values of Eq. (39), may be interpreted as a components intersection. The information on the occurrence of a components intersection allows the correct determination of the local number of time supported components. By combining this information with the total number of rising edges of $N(p)$, the total number of components in a signal can be obtained.

Fig. 8 shows an example of a signal with crossing components, corresponding to a radar signal obtained from a rotating object. The local number of estimated components $N(p)$ presents fast changes when the components intersect, producing large values of $|a(p)|$, which in return indicate the time occurrences of the components intersections.

3.2.2. Performance analysis in noise

The previous example shows that in ideal (non-noisy) conditions the estimated values of $a(p)$ in case of components starting/ending are in accordance with Eqs. (37), (38). However, the presence of noise can alter the estimation of the number of components $N(p)$ [3], and thus influence its derivative $a(p)$. Fig. 9 shows the spectrograms of the signals from Figs. 5, 6 embedded in AWGN ($SNR = 10$ dB), showing that the presence of noise has brought variations in the estimation results. The function $a(p)$ for

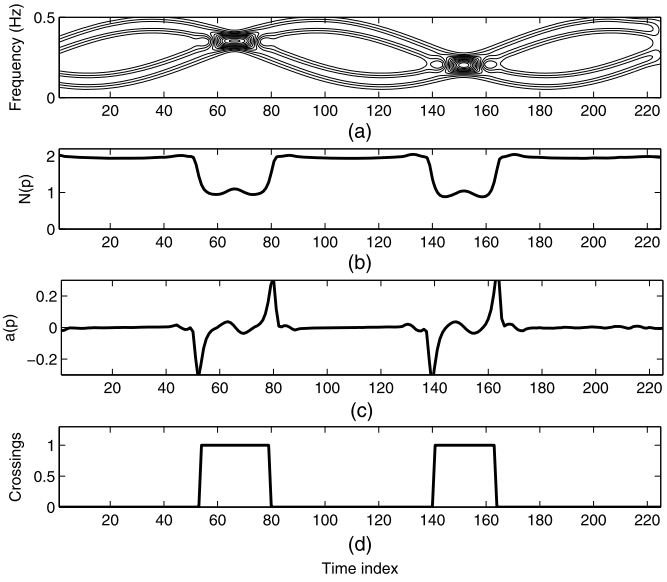

Fig. 8. Spectrogram of a signal with crossing components (a), local number of components $N(p)$ (b), derivative $a(p)$ (c), detection of components crossings (d).

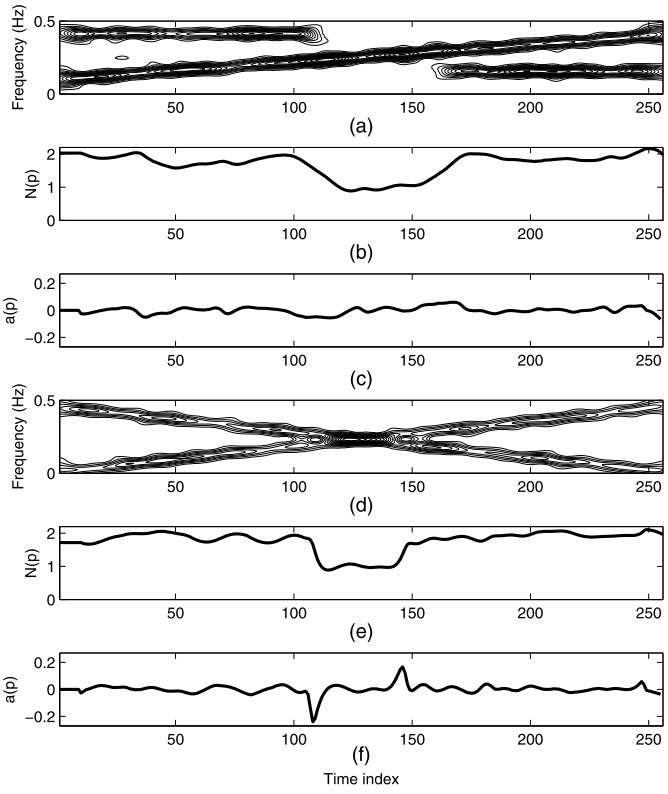

Fig. 9. Spectrogram of a noisy signal with truncated components (a), local number of components $N(p)$ (b), derivative $a(p)$ (c), spectrogram of a noisy signal with crossing components (d), local number of components $N(p)$ (e), derivative $a(p)$ (f).

both cases presents fluctuations which are not correlated to components starts/ends, or intersections locations. However, the occurrence of the components crossing is still prominently marked in the function $a(p)$, Fig. 9(f). This suggests that in applications involving noisy signals, a numerical criterium for the detection of components intersections can be adapted by treating as an intersection mark each value of $|a(p)|$ exceeding a less restrictive version of Eq. (39). Since in non-noisy conditions the values of $|a(p)|$ in the case of intersections are typically at least two times larger

Table 1
False detection probability.

SNR dB	Probability of false detection [%]
7	4.83
10	1.96
12	1.17
15	0.5

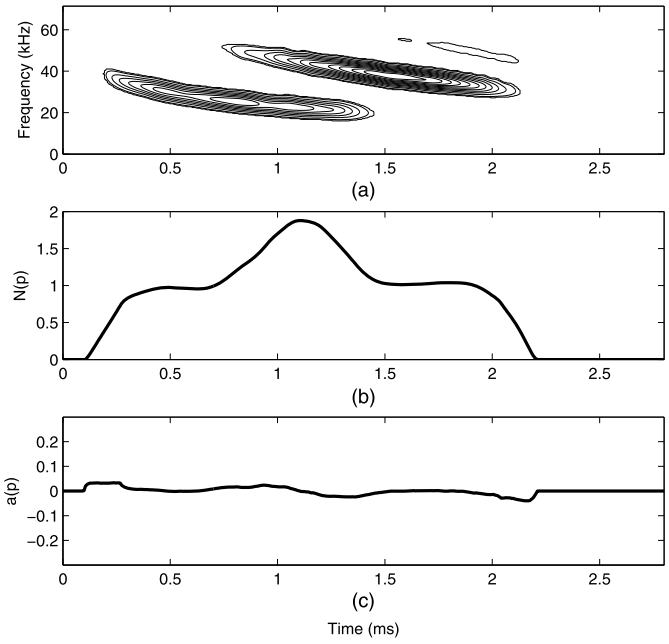

Fig. 10. Spectrogram of a bat echo-location signal (a), local number of components $N(p)$ (b), numerical derivative $a(p)$ (c).

than the value obtained from Eq. (39), we propose the threshold for intersections detection to be $a_t = A/\Delta t$, with A chosen between 1.5 and 2.

In order to validate the proposed criterion, simulations (including 600 different noisy signal realizations presenting intersections or ending/starting components) have been run for four levels of noise. The probabilities of false detection are reported in Table 1. The results in Table 1 show that for $SNR = 7$ dB the probability of false detection, based on the threshold $a_t = 1.75/\Delta t$, is below 5%, and rapidly decreasing as the noise level decreases. Based on the obtained results, the proposed threshold a_t can be used as a reliable indicator of components intersection in moderate noise conditions.

4. Real data experiments

The performance of the local Rényi entropy as a detector of the signal components time supports will be next validated on real-life signals.

4.1. Natural sonar

Figs. 10 and 11 show the local entropy estimates of the spectrogram of bat echolocation signals. The signal in Fig. 10[1] has a duration $D = 400$ samples, with the entropy analysis interval $\Delta t = round(D/17) = 24$ samples, and the sampling frequency $f_s = 142.857$ kHz. From the estimation results, it can be seen that the time supports of the dominant components are consistent with the local component content of the spectrogram. Also, the components beginnings and endings cause linear behavior of $N(p)$, producing the derivative extrema $max(a(p)) = 0.03336$, and $min(a(p)) = -0.03985$ for the considered Δt.

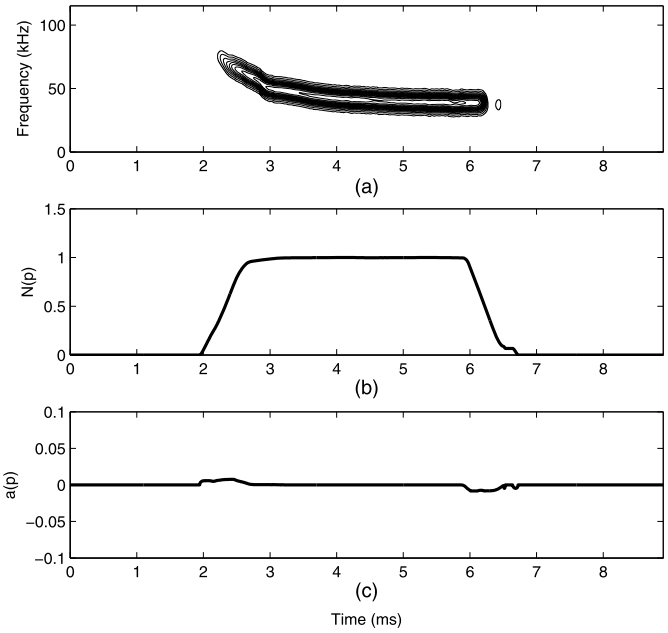

Fig. 11. Spectrogram of a bat echo-location signal (a), local number of components $N(p)$ (b), numerical derivative $a(p)$ (c).

Fig. 11 shows the spectrogram of a bat echolocation signal of duration $D = 2048$ samples, with $\Delta t = round(D/17) = 120$ samples, and $f_s = 230.4$ kHz. Again, the function $N(p)$ correctly detects the time support of the component, with quasi-linear behavior at the component beginning and ending. The extreme values of $a(p)$ are $max(a(p)) = 0.00756$, and $min(a(p)) = -0.00829$.

4.2. EEG data

The local Rényi entropy estimation has been applied to EEG data. As shown in Figs. 12, 13, 14, and 15 EEG signals can simultaneously present dominant components and low amplitude components. As a result of such an instantaneous amplitude difference, lower amplitude components bring smaller contributions to the total number of components $N(p)$, as shown in [17]. The signal in Fig. 12 has a duration $D = 256$ samples, with the entropy analysis interval $\Delta t = round(D/17) = 15$ samples, and the sampling frequency $f_s = 20$ Hz. The extreme values of $a(p)$ are $max(a(p)) = 0.08496$, and $min(a(p)) = -0.05981$. The signal in Fig. 13 has a duration $D = 591$ samples, $\Delta t = round(D/17) = 35$ samples, and $f_s = 20$ Hz, with $max(a(p)) = 0.01173$ and $min(a(p)) = -0.02696$. The signals in Figs. 14 and 15 have $D = 512$ samples, $\Delta t = round(D/17) = 30$ samples, and $f_s = 20$ Hz, and $max(a(p)) = 0.05768$ and $min(a(p)) = -0.04647$. So, even though the presence of low energy components influences the estimation, the results are consistent with what has been observed in the signal spectrogram.

Note that an alternative approach for $N(p)$ estimation was introduced in [17]. The approach was developed to be used with signals having non-equal amplitude components, such as the EEG data analyzed in this paper.

5. Discussion and conclusion

In many applications, it is important to estimate the local number of components in a nonstationary signal. A valuable alternative

[1] The authors wish to thank Curtis Condon, Ken White, and Al Feng of the Beckman Institute of the University of Illinois for the bat data and for permission to use it in this paper.

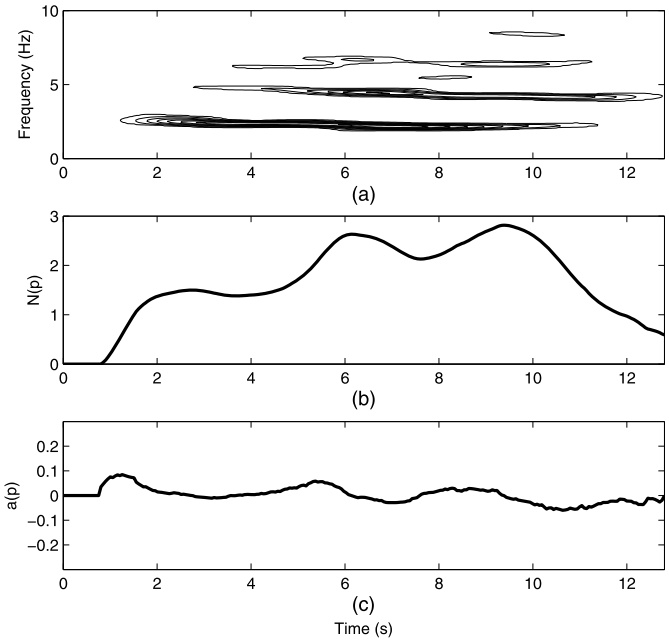

Fig. 12. Spectrogram of an EEG signal (a), local number of components $N(p)$ (b), derivative $a(p)$ (c).

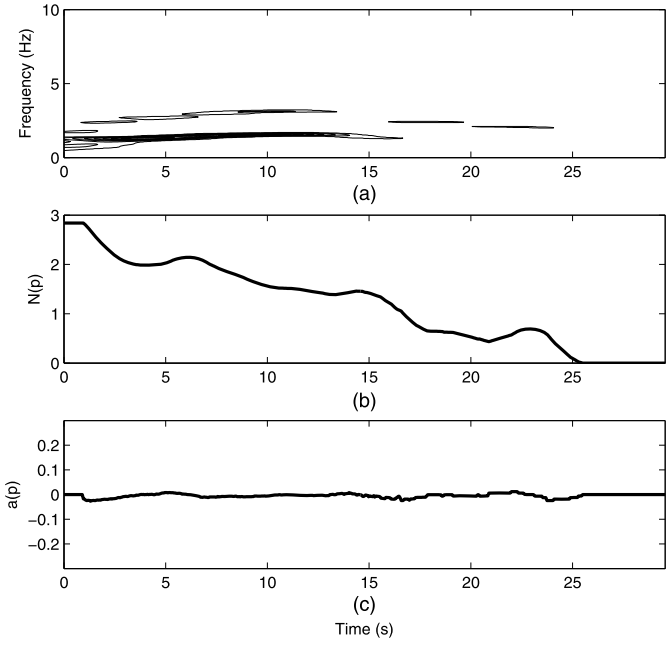

Fig. 13. Spectrogram of an EEG signal (a), local number of components $N(p)$ (b), derivative $a(p)$ (c).

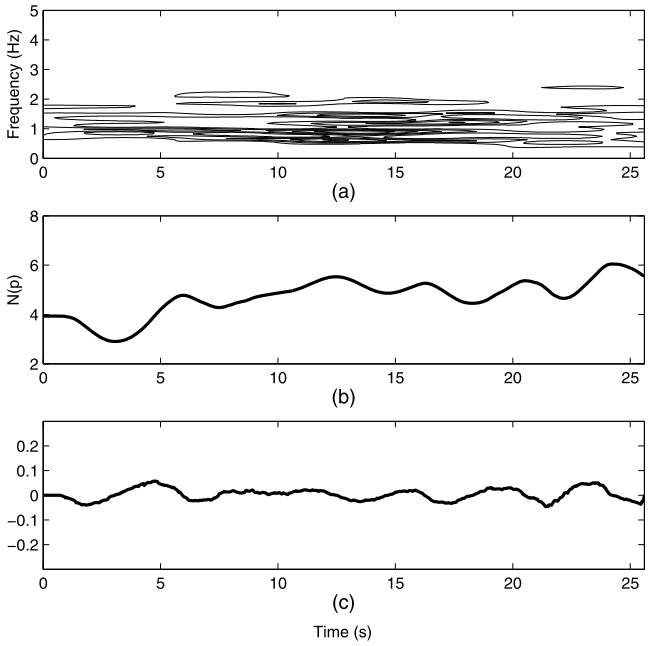

Fig. 14. Spectrogram of an EEG signal (a), local number of components $N(p)$ (b), derivative $a(p)$ (c).

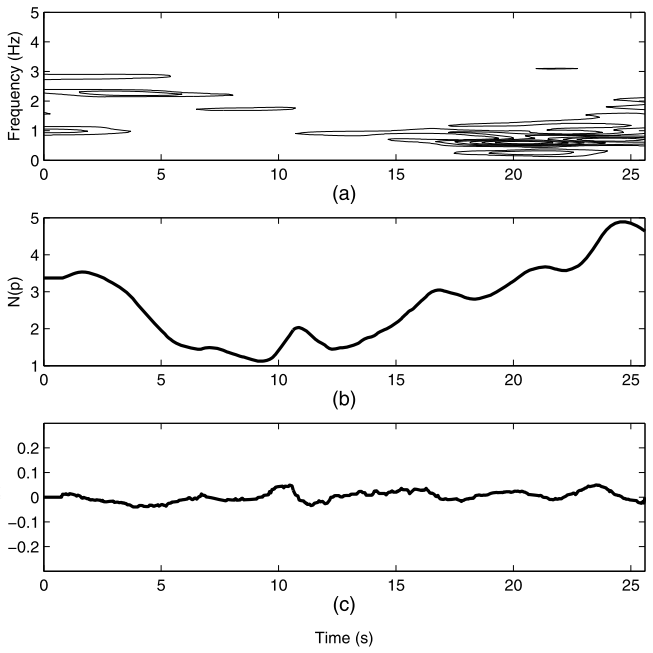

Fig. 15. Spectrogram of an EEG signal (a), local number of components $N(p)$ (b), derivative $a(p)$ (c).

to other estimation methods based on TFDs was provided in [3] using the Short-term Rényi entropy. Unlike the classic methods for estimation of the local number of signal components, which involve counting the peaks in the (t, f) plane at each time instant for as long as the peak amplitude exceeds a fixed threshold, the estimation based on the Short-term Rényi entropy detects a component whenever it locally presents the entropy characteristics of the reference signal [3].

The presented analysis of the Short-term Rényi entropy estimation when applied to the spectrogram clarifies the effect TFD parameters and the entropy order have on the obtained results. Even though the Short-term Rényi entropy generally increases with the time estimation interval, and decreases by increasing the standard deviation of the spectrogram window and the entropy order, the estimated number of components is invariant to these parameters, under the assumption of components being separated in the time-frequency plane.

The counting property of the Short-term Rényi entropy is extended to nonstationary signals, and important new insights on the signal structure, reveling components crossings and components ending/starting times, are obtained when the features of the entropy-based estimated number of components are analyzed. The presented approach allows for the resolving of ambiguities in the case of local decrements of the number of components. The information on the time locations of components crossings can be combined with the entropy-based estimate of the number of com-

ponents for a correct estimation of the total and local number of supported components. Simulations on synthetic signals in moderate noise and real data show that the estimation results can be used as reliable inputs needed by blind source separation procedures in multicomponent IF estimation applications [2,16].

Knowing the number of components locally supported in time and the global number of components present in the signal improves memory allocation in numerical simulations. The estimated number of components determines the total allocated memory and the momentarily used memory block. Dynamic strategy of memory usage avoids blind allocation and decreases the algorithm execution time. Using the information on the number of components present in a signal, and dynamic memory allocation, situations leading to incomplete components extraction (whenever the number of existing components is larger than the arbitrarily assumed one) or memory overflow are less likely to occur.

Acknowledgments

This study is a part of the research project "Optimization and Design of Time-Frequency Distributions" (No. 069-0362214-1575), which was financially supported by the Ministry of Science, Education and Sports of the Republic of Croatia.

The third author would like to acknowledge funding for a part of this research by Qatar Foundation under grant NPRP 06-885-2-364.

Appendix A

A.1. Proof 1

If a pure tone is considered, $x(t) = e^{j2\pi f_0 t}$, the spectrogram with a Gaussian window $w(t) = (\pi\sigma^2)^{-1/4} e^{-t^2/2\sigma^2}$, will take the form:

$$
\begin{aligned}
&STFT_x(t,f) \\
&= \int_{-\infty}^{\infty} x(\tau) w(\tau - t) e^{-j2\pi f\tau} d\tau \\
&= \int_{-\infty}^{\infty} e^{j2\pi f_0\tau} (\pi\sigma^2)^{-1/4} e^{-(\tau-t)^2/2\sigma^2} e^{-j2\pi f\tau} d\tau \\
&= (\pi\sigma^2)^{-1/4} \int_{-\infty}^{\infty} e^{-\left(\frac{\tau^2 - 2t\tau + t^2 + j4\pi\sigma^2\tau(f-f_0)}{2\sigma^2}\right)} d\tau \\
&= (\pi\sigma^2)^{-1/4} \int_{-\infty}^{\infty} e^{-\left(\frac{\tau^2 - 2\tau(t - j2\pi\sigma^2(f-f_0)) + t^2}{2\sigma^2}\right)} d\tau \\
&= (\pi\sigma^2)^{-1/4} \\
&\quad \times \int_{-\infty}^{\infty} e^{\left(-\frac{[\tau - (t - j2\pi\sigma^2(f-f_0))]^2}{2\sigma^2} - j2\pi t(f-f_0) - 2\pi^2\sigma^2(f-f_0)^2\right)} d\tau \\
&= (\pi\sigma^2)^{-1/4} e^{-j2\pi(f-f_0)t} e^{-2\pi^2\sigma^2(f-f_0)^2} \\
&\quad \times \int_{-\infty}^{\infty} e^{-\frac{[\tau - (t - j2\pi^2\sigma^2(f-f_0))]^2}{2\sigma^2}} d\tau \\
&= (\pi\sigma^2)^{-1/4} \sqrt{2\sigma^2\pi}\, e^{-j2\pi(f-f_0)t} e^{-2\pi^2\sigma^2(f-f_0)^2}
\end{aligned}
\tag{A.1}
$$

A.2. Proof 2

For the spectrogram defined as

$$S_x(t,f) = K e^{-4\pi^2\sigma^2(f-f_0)^2},$$

the Short-term Rényi entropy will be

$$
\begin{aligned}
H_{\alpha,x}(p) &= \frac{1}{1-\alpha} \log_2 \frac{\int_{p-\Delta t/2}^{p+\Delta t/2} \int_{-\infty}^{\infty} (K e^{-4\pi^2\sigma^2(f-f_0)^2})^\alpha dt df}{(\int_{p-\Delta t/2}^{p+\Delta t/2} \int_{-\infty}^{\infty} K e^{-4\pi^2\sigma^2(f-f_0)^2} dt\, df)^\alpha} \\
&= \frac{1}{1-\alpha} \log_2 \frac{K^\alpha \int_{p-\Delta t/2}^{p+\Delta t/2} \int_{-\infty}^{\infty} e^{-4\pi^2\sigma^2\alpha(f-f_0)^2} dt df}{K^\alpha (\int_{p-\Delta t/2}^{p+\Delta t/2} \int_{-\infty}^{\infty} e^{-4\pi^2\sigma^2(f-f_0)^2} dt df)^\alpha} \\
&= \frac{1}{1-\alpha} \log_2 \frac{\int_{p-\Delta t/2}^{p+\Delta t/2} \sqrt{\frac{\pi}{4\alpha\pi^2\sigma^2}} e^{\left(\frac{64\alpha^2\pi^4\sigma^4 f_0^2 - 64\alpha^2\pi^4\sigma^4 f_0^2}{16\alpha\pi^2\sigma^2}\right)} dt}{(\int_{p-\Delta t/2}^{p+\Delta t/2} \sqrt{\frac{\pi}{4\pi^2\sigma^2}} e^{\left(\frac{64\pi^4\sigma^4 f_0^2 - 64\pi^4\sigma^4 f_0^2}{16\pi^2\sigma^2}\right)} dt)^\alpha} \\
&= \frac{1}{1-\alpha} \log_2 \frac{\sqrt{\frac{1}{4\alpha\pi\sigma^2}}\Delta t}{(\sqrt{\frac{1}{4\pi\sigma^2}}\Delta t)^\alpha} \\
&= \log_2 \Delta t + \log_2 \frac{1}{2\sqrt{\pi}\sigma} \alpha^{-\frac{1}{2(1-\alpha)}}.
\end{aligned}
\tag{A.2}
$$

Appendix B. Supplementary material

Supplementary material related to this article can be found online at http://dx.doi.org/10.1016/j.dsp.2014.07.013.

References

[1] B. Boashash, Time Frequency Signal Analysis and Processing: A Comprehensive Reference, Elsevier, Oxford, UK, 2003.
[2] B. Boashash, Estimating and interpreting the instantaneous frequency of a signal—part 1: fundamentals; part 2: algorithms and applications, Proc. IEEE 80 (1992) 519–568.
[3] V. Sucic, N. Saulig, B. Boashash, Estimating the number of components of a multicomponent nonstationary signal using the short-term time-frequency Rényi entropy, EURASIP J. Adv. Signal Process. 2011 (2011) 125, http://dx.doi.org/10.1186/1687-6180-2011-125.
[4] B. Barkat, K. Abed-Meraim, Algorithms for blind components separation and extraction from the time-frequency distribution of their mixture, EURASIP J. Appl. Signal Process. 13 (2004) 2025–2033.
[5] B. Boashash, V. Sucic, Resolution measure criteria for the objective assessment of the performance of quadratic time-frequency distributions, IEEE Trans. Signal Process. 51 (2003) 1253–1263.
[6] Lj. Stankovic, S. Stankovic, An analysis of instantaneous frequency representation using time-frequency distributions-generalized Wigner distribution, IEEE Trans. Signal Process. 43 (2) (1995) 549–552.
[7] Lj. Stankovic, A method for time-frequency analysis, IEEE Trans. Signal Process. 42 (1) (1994) 225–229.
[8] Z.M. Hussain, B. Boashash, Adaptive instantaneous frequency estimation of multicomponent FM signals using quadratic time-frequency distributions, IEEE Trans. Signal Process. 50 (8) (2002) 1866–1876.
[9] Lj. Stankovic, S-class of time-frequency distributions, IEE Proc., Vis. Image Signal Process. 144 (2) (1997) 57–64.
[10] S. Stankovic, N. Zaric, I. Orovic, C. Ioana, General form of the time-frequency distribution with complex-lag argument, Electron. Lett. 44 (11) (2008) 699–701.
[11] E. Sejdić, I. Djurović, J. Jiang, Time-frequency feature representation using energy concentration: an overview of recent advances, Digit. Signal Process. 19 (2009) 153–183.
[12] A. Rényi, On measures of entropy and information, in: Proc. 4th Berkeley Symp, in: Mathematics of Statistics and Probability, vol. 1, 1961, pp. 547–561.
[13] R.G. Baraniuk, P. Flandrin, A.J.E.M. Janssen, O.J.J. Michel, Measuring time-frequency information content using the Renyi entropies, IEEE Trans. Inf. Theory 47 (4) (2001) 1391–1409.
[14] N. Saulig, V. Sucic, S. Stanković, I. Orović, B. Boashash, Signal content estimation based on the short-term time-frequency Rényi entropy of the S-method time-frequency distribution, in: 19th International Conference on Systems, Signals and Image Processing (IWSSIP), Vienna, 2012.

[15] S. Kadambe, G.F. Boudreaux-Bartels, A comparison of the existence of 'cross terms' in the Wigner distribution and the squared magnitude of the wavelet transform and the short-time Fourier transform, IEEE Trans. Signal Process. 40 (10) (Oct 1992) 2498–2517, http://dx.doi.org/10.1109/78.157292.
[16] J. Lerga, V. Sucic, B. Boashash, An efficient algorithm for instantaneous frequency estimation of nonstationary multicomponent signals in low SNR, EURASIP J. Adv. Signal Process. 2011 (2011) 725189, http://dx.doi.org/10.1155/2011/725189.
[17] N. Saulig, N. Pustelnik, P. Borgnat, P. Flandrin, V. Sucic, Instantaneous counting of components in nonstationary signals, in: 21st European Signal Processing Conf., EUSIPCO-13, Marrakech, 2013.

Victor Sucic received BS and PhD degrees in Electrical and Computer Engineering from Queensland University of Technology, Brisbane, Australia, in 1998 and 2004, respectively. Since 2005, he has been with the Faculty of Engineering, University of Rijeka, Croatia, where he is the Signals and Systems Chair. Professor Sucic has authored over 50 research publications, including three book chapters and over ten papers in leading signal processing journals. His main research interests are time-frequency signal analysis and statistical signal analysis and processing.

Nicoletta Saulig received her MS degree in Electrical Engineering from the Faculty of Engineering, University of Rijeka, Croatia, in 2009. She is currently working toward the PhD degree at the Faculty of Electrical Engineering and Computing, University of Zagreb, Croatia. Her field of interest is time-frequency signal analysis.

Boualem Boashash (IEEE Fellow 99) is a Scholar and Senior Academic with experience in 5 leading Universities in France and Australia. He has published over 500 technical publications, including over 100 journal publications covering Engineering, Applied Mathematics and Bio-medicine. He pioneered the field of Time-Frequency Signal Processing.